Computer-Aided Generation of Escher-like Sky and Water Tiling Patterns

Computer-Aided Generation of Escher-like Sky and Water Tiling Patterns

Kokichi Sugihara*
Meiji University, 4-21-1 Nakano, Nakano-ku, Tokyo 164-8525, Japan
kokichis@meiji.ac.jp

Abstract Dutch graphic artist M. C. Escher created many interesting prints based on tiling patterns. A typical example of such a print is *Sky and Water I*, in which a bird at the top deforms gradually towards the bottom and melts away into the background, while a fish gradually appears from the background. This paper presents an interactive system for creating Escher-like Sky and Water tiling patterns. In this system, a user supplies two figures, and the system places deformed copies of them in such a way that, from top to bottom, one figure gradually disappears into the background, while the other figure gradually appears from the background. The system combines tiling, morphing, and figure-ground reversal. The user can also specify the density of and a global pattern for the tiling.

Keywords: tiling, morphing, Escher, figure-ground reversal, optical illusion.

AMS MSC Code: 68U05

1 Introduction

M. C. Escher (1898–1972), a Dutch graphic artist, created many interesting works based on tiling. A typical class of tiling art is based on isohedral tiling, in which identical tiles are placed so that the plane is covered without gaps or overlaps and each tile is surrounded in the same manner. For this class of tiling, possible patterns can be enumerated using a group-theoretic approach, and the complete list of 17 symmetry groups and the complete list of 93 types of incidence structure for tile boundaries have been constructed [6, 10]. These lists have been used to analyze Escher's work from a mathematical point of view [3, 11, 13], and interactive systems for creating them have also been proposed [2, 8, 9]. This class of tiling art has been well studied mathematically, from both the analytic and synthetic points of view, perhaps because isohedral tiling is a purely mathematical topic in itself.

Another class of Escher's tiling art is based on gradually deforming tiles. Escher used various deformation variations, and Kaplan (2008) classified them into six types of transition, namely realization,

*This manuscript was published in *Journal of mathematics and the Arts*, vol. 3, no. 4 (2009), pp. 195–207.

crossfade, abutment, growth, sky-and-water, and interpolation. He also pointed out that all six types are used in *Metamorphosis II and Metamorphosis III.* Moreover, the table in his paper [7] suggests that the sky-and-water type and the interpolation type are used more often than the other four types.

In this paper, we concentrate on the fifth type, namely the sky-and-water type. A typical example of this type is *Sky and Water I* (1938), as shown in Figure 1, where a bird is placed at the top, a fish at the bottom, and there are several tiles in between so that the bird shape continuously deforms downwards, melting away into the background, and the fish gradually appears from the background [11]. As Teuber (1986) has pointed out, this class of art is a mixture of tile packing, figure-ground reversal, and gradual deformation of figures (see also [4]). In this sense, this class of tiling art does not have a purely mathematical structure, but is a mixture of mathematics and other areas that are more vague. Because of its nature, this class of tiling art has not been studied from a mathematical point of view as rigorously as other tiling art such as isohedral tiling art.

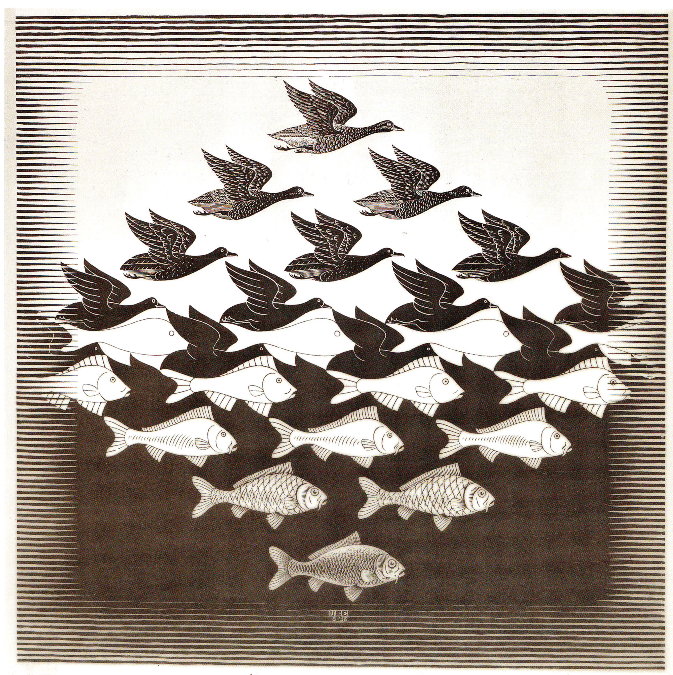

Figure 1. M. C. Escher's "Sky and Water I"©2009 The M. C. Escher Company-Holland. All rights reserved. www.mcescher.com

Recently, Schattschneider (2008) has studied the figure-ground aspect of Escher's art in terms of "duality", which describes the property that the tiles are assigned one of two colors so that tiles sharing an edge have different colors from each other. If we pay attention to one of these colors, the tiles with the other color are perceived to be part of the background. She classified two-colored monohedral and dihedral tilings into three categories according to the color assignment patterns [12]. Although she concentrated on tilings without transitional deformation, she pointed out that *Sky and Water I* is a typical example in which the duality and individuality of tiles are emphasized.

In this paper, we consider how to create Sky and Water tiling patterns automatically for an arbitrary pair of figures. Escher (and later, Kaplan and Salesin [8]) create Sky and Water designs from the "inside out"— first they develop a central tiling that matches the two goal shapes, and then deform above and below to the shapes. This paper works from the "outisde in"— it starts with the goal shapes and finds a best compromise interface between them.

The basic graphical technique we use is morphing [1, 5], but it is not trivial to apply this technique to our problem. This is because the original morphing technique was for deformation from one figure to another, whereas our goal is the deformation from a figure to the background, and from the background to a second figure. We present a method for applying the morphing technique to this requirement, together with computer-generated examples.

We would emphasize that the primary aim of this paper is in developing an engineering technique. That is, we are interested in constructing a computer-aided system that helps designers to create their own patterns. The patterns created by this system are inspired by Escher's *Sky and Water I*, but they are not necessarily faithful simulations of Escher's method. We will first propose our method, then observe the behavior of our system, and finally compare the outputs of our system with Escher's Sky and Water patterns.

2 Figure-Background Morphing

2.1 Basic Idea

Suppose that we are given two tiles A and B and we want to generate a Sky and Water pattern using these tiles.

For this purpose, we consider an $(n+1) \times n$ black-and-white checkerboard of rhombuses as shown in Figure 2. Without loss of generality, assume that the top rhombus is colored white. Because the number of rhombuses along one side differs by one from that along the other side, the color of the bottom rhombus is black. Place the tile A and its deformed copies in white rhombuses and the tile B and its deformed copies in black rhombuses.

We want to deform the tiles A and B so that they gradually melt away into the background. To achieve this, we apply morphing techniques to the tile A and the pattern generated as a vacant space surrounded by copies of the pattern B. The procedure comprises the following six steps, and a detailed

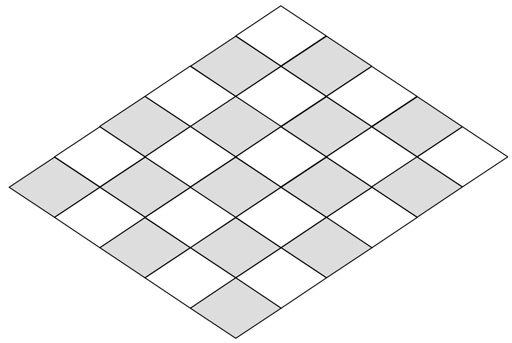

Figure 2. Checkerboard pattern for tile placement.

description of these steps will be given in the next and later subsections.

Step 1. Choose a rhombus shape that closely fits both tiles A and B.

Step 2. Construct the shape, say shape C, that is formed by four copies of the tile B around a single white rhombus in the checkerboard.

Step 3. Generate a sequence of continuous deformations from the tile A to the shape C.

Step 4. Place the sequence of deformed tiles in the columns of the white rhombuses in the checkerboard.

Step 5. Reconnect the boundary segments of the deformed tiles so that the tile A and its deformed copies are visible in the upper part of the checkerboard and the tile B and its deformed copies are visible in the lower part.

Step 6. Paint the tiles and the background.

In the following sections, we discuss each step in more detail.

2.2 Adjustment of the Tile Sizes

Suppose that the tiles A and B are represented by closed sets of points. Let $x_{\max}(A)$ be the maximum of the x coordinates of the points on the boundary of A. Similarly, let $x_{\min}(A)$, $y_{\max}(A)$, and $y_{\min}(A)$ be the minimum x coordinate, the maximum y coordinate, and the minimum y coordinate, respectively, of the boundary of A. We define

$$w(A) = x_{\max}(A) - x_{\min}(A), \tag{1}$$

$$h(A) = y_{\max}(A) - y_{\min}(A), \tag{2}$$

and call them the *width* and the *height* of A, respectively. We also define the center of A as

$$\left(\frac{x_{\max}(A) + x_{\min}(A)}{2}, \frac{y_{\max}(A) + y_{\min}(A)}{2} \right). \tag{3}$$

The width, the height, and the center of the other shape B are defined similarly.

Next, let r be the average of $h(A)/w(A)$ and $h(B)/w(B)$, and let R be a rhombus with height r and width 1. That is, R is a rhombus whose height-to-width ratio is equal to the average of those of A and B. This completes Step 1.

We now adjust the sizes of A and B by scale transformations, so that they are contained within a rectangle of height r and width 1 and are the largest having this property.

From now on, we assume that tiles A and B are always accompanied by the rhombus R with the same center.

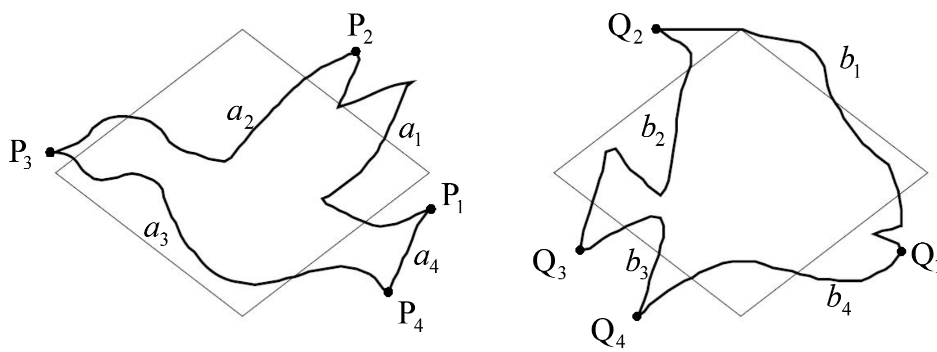

(a) Tile A (b) Tile B

Figure 3. Pair of scale-adjusted tiles.

Figure 3 shows an example of a pair of scale-adjusted tiles A and B accompanied by the rhombus R. In what follows, we use this pair of tiles to describe the proposed method.

2.3 Construction of the Vacant Space

Our next task is to construct the shape of the vacant space that is formed by four copies of the tile B around a single white rhombus on the checkerboard. To achieve this, we partition the boundary curves of the tiles into four segments. We consider the rhombus as the basic tile shape with its four vertices at the top, the bottom, the right, and the left. Therefore, we also partition the boundary of a given tile at the top, the bottom, the rightmost, and the leftmost points.

As shown in Figure 3(a), let $\mathrm{P}_1, \mathrm{P}_2, \mathrm{P}_3$, and P_4 be the rightmost, the top, the leftmost, and the bottom points of A. These points may not be unique. If the rightmost point is not unique, we choose as P_1 the point that is closest to the rightmost vertex of the rhombus R. A similar convention is adopted for the points $\mathrm{P}_2, \mathrm{P}_3$, and P_4 if they are not unique. We assume that the resulting four points are all distinct.

We partition the boundary of the tile A into four segments, delimited by $\mathrm{P}_1, \mathrm{P}_2, \mathrm{P}_3$, and P_4. Let the segment from P_1 to P_2 be represented by the curve $a_1(s), 0 \leq s \leq 1$, using the parameter s. That is, a_1 is the mapping from the interval $[0,1]$ to the plane such that, as s moves from 0 to 1 continuously, $a_1(s)$ traces the segment of the boundary of the tile A from P_1 to P_2 counterclockwise. Similarly, we define $a_2(s), a_3(s)$, and $a_4(s), 0 \leq s \leq 1$, as the curves corresponding to the segments of the boundary of A from P_2 to P_3, from P_3 to P_4, and from P_4 to P_1, respectively. Therefore,

$$\begin{aligned} &a_1(0) = a_4(1) = \mathrm{P}_1, \quad a_1(1) = a_2(0) = \mathrm{P}_2, \quad a_2(1) = a_3(0) = \mathrm{P}_3, \\ &a_3(1) = a_4(0) = \mathrm{P}_4. \end{aligned} \tag{4}$$

As shown in Figure 3(b), the boundary of the tile B is also partitioned into four segments at the rightmost point Q_1, the top point Q_2, the leftmost point Q_3, and the bottom point Q_4. Let the resulting curves be represented by $b_1(s)$, $b_2(s)$, $b_3(s)$, and $b_4(s)$, $0 \leq s \leq 1$, such that the curve $b_1(s)$ represents the segment from Q_1 to Q_2, $b_2(s)$ from Q_2 to Q_3, $b_3(s)$ from Q_3 to Q_4, and $b_4(s)$ from Q_4 to Q_1.

Next, as shown in Figure 4, we place four copies of B in such a way that the accompanying four rhombuses form a checkerboard pattern surrounding a common rhombus. We collect the segments of the boundary curves facing the common rhombus at the center. The resulting collection of four segments can be regarded as the representation of the vacant space surrounded by the copies of B in counterclockwise order b_3, b_4, b_1, and b_2.

The vacant space is to the right of each curve b_i. So we reverse the direction of the curves and define the resulting segments by

$$\begin{aligned} \bar{b}_1(s) &= (-1/2, -r/2) + b_1(1-s), \\ \bar{b}_2(s) &= (+1/2, -r/2) + b_2(1-s), \\ \bar{b}_3(s) &= (+1/2, +r/2) + b_3(1-s), \\ \bar{b}_4(s) &= (-1/2, +r/2) + b_4(1-s), \end{aligned} \tag{5}$$

where the first term in each right-hand side represents a translation (recall that the width of the rhombus is 1 and the height is r) and the second term reverses the direction of the curve. Note that these segments do not necessarily form a closed curve. For example, the end point $\bar{b}_1(1)$ of the first segment does not coincide with the start point $\bar{b}_2(0)$ of the second segment, in general. However, this does not cause a problem in our case, in the sense that the subsequent steps of the procedure can be executed no matter how distant the four segments are from each other. The quality of the resulting pattern, on the other hand, does depend on the configuration of the segments. We will discuss this issue further, in Subsection

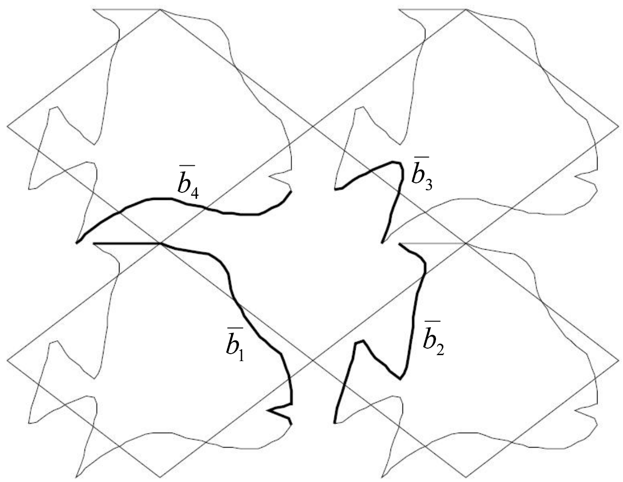

Figure 4. Vacant space surrounded by four tiles.

3.1. We denote as *shape* C the collection of segments $\bar{b}_1(s), \bar{b}_2(s), \bar{b}_3(s)$, and $\bar{b}_4(s)$. This completes Step 2.

2.4 Morphing from the Tile to the Vacant Space

We next generate a continuous deformation from the tile A to the vacant space C. Here, we apply the morphing technique to the four pairs of the associated segments of A and C. For example, the simplest way is to apply a linear morphism, from which we obtain

$$\begin{array}{l} c_1(s,t) = (1-t)a_1(s) + t\bar{b}_3(s), \\ c_2(s,t) = (1-t)a_2(s) + t\bar{b}_4(s), \\ c_3(s,t) = (1-t)a_3(s) + t\bar{b}_1(s), \\ c_4(s,t) = (1-t)a_4(s) + t\bar{b}_2(s), \end{array} \tag{6}$$

where the new parameter t varies as $0 \leq t \leq 1$. Note that, if $t = 0$, $c_i(s,t)$ coincides with $a_i(s)$, and if $t = 1$, $c_i(s,t)$ coincides with $\bar{b}_{i+2}(s)$, where $\bar{b}_5$ and $\bar{b}_6$ should be read as $\bar{b}_1$ and $\bar{b}_2$, respectively.

The linear morphism defined by equations (6) is the simplest possible, and this morphism might generate self-intersection if the corresponding two curves differ too much. However, there are many sophisticated nonlinear morphisms [1, 5], and we can use them if the linear morphism proves unsatisfactory.

Next, we fix $t_1 = 0 < t_2 < t_3 < \cdots < t_n = 1$, and construct the sequence of deformed patterns $c_i(s,t_j)$, $i = 1,2,3,4, j = 1,2,\cdots,n$. This completes Step 3.

Figure 5 shows the sequence of deformed boundary segments for the example tile A in Figure 3(a) and the vacant space in Figure 4.

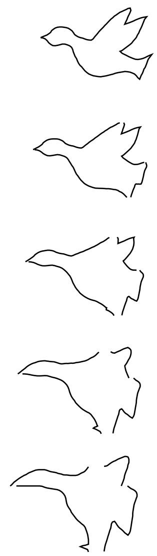

Figure 5. Morphing from the tile A to the vacant space.

2.5 Placement of Tiles

The original tile A (i.e., $c_i(s, t_1)$) is placed on the top white rhombus. Then place the deformed tiles $c_i(s, t_j)$ on the white rhombuses of the checkerboard from the top downwards. Copies of the second deformed pattern $c_i(s, t_2)$ are placed on the white rhombuses in the next row. Similarly, the copies of the jth deformed pattern $c_i(s, t_j)$ are placed on the white rhombuses in the jth row from the top. This completes Step 4.

Figure 6 shows the result of this step for the example pair of tiles in Figure 3 placed on the checkerboard in Figure 2.

Next, we reconnect the curves so that, in the upper half of the checkerboard, the tiles at the white rhombuses are represented by closed curves, while, in the lower half, the tiles at the black rhombuses are represented by closed curves. In this way, we connect the end point of the ith segment $c_i(s, t_j)$ and the start point of the $(i + 1)$st segment $c_{i+1}(s, t_j)$ in the upper half of the checkerboard. In the lower half of the checkerboard, on the other hand, we connect the terminal points of the four segments so that the tiles at the black rhombuses are represented by closed curves. More specifically, the start point of c_1 is connected to the end point of c_2 of its right neighbor tile, the end point of c_1 is connected to the start point of c_3 of its upper neighbor tile, the start point of c_2 is connected to the end point of c_3 of its upper neighbor tile, the end point of c_2 is connected to the start point of c_1 at its left neighbor tile, and so on.

Finally, we move the tiles apart from each other slightly so that the distinction between the figures and the background becomes clearer. This completes Step 5.

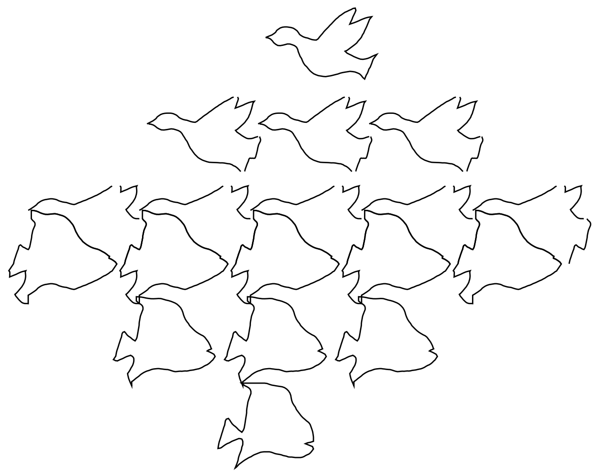

Figure 6. Placement of the boundary segments of the morphing patterns.

Figure 7 shows the result of Step 5 for the example pair of the tiles.

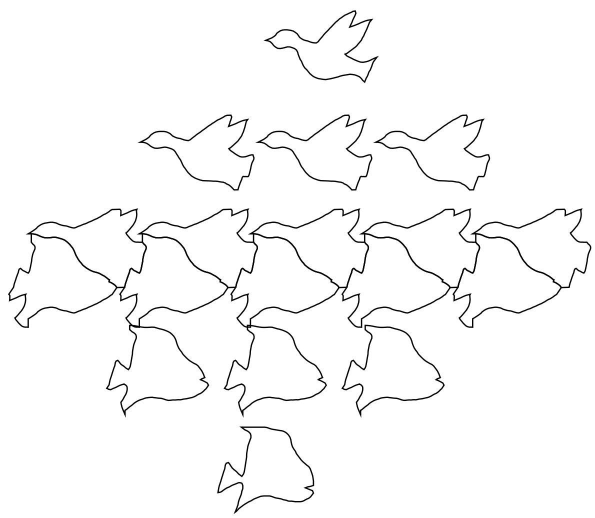

Figure 7. Sky and Water pattern generated by the proposed method.

2.6 Painting

We paint the tiles and the background in a monochrome tone. To achieve this, we first choose a color to paint, and then assign this color to the background in such a way that the brightness is the highest at the top and gradually decreases downwards.

For the tiles, on the other hand, we paint the lowest tile most brightly, and decrease the brightness

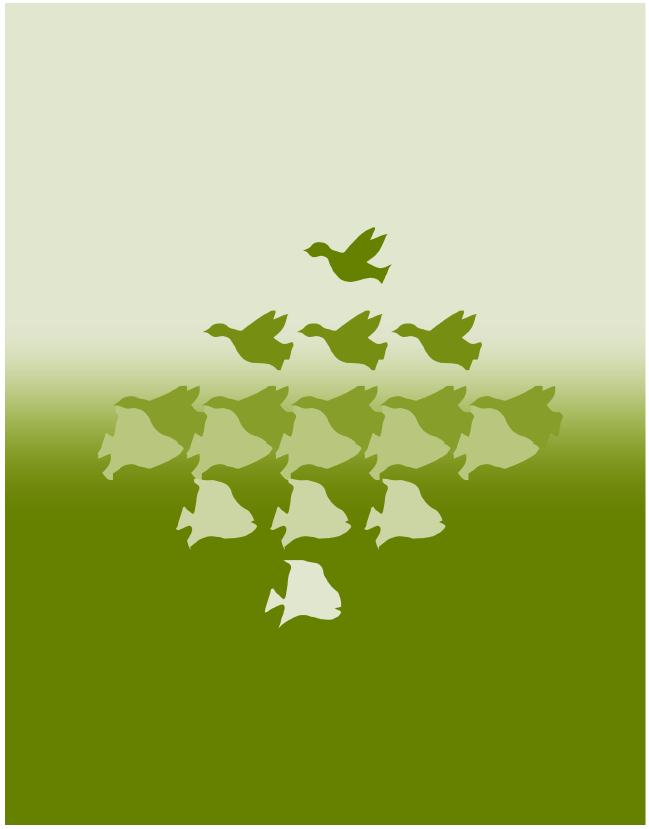

Figure 8. Final result of painting.

gradually upwards. This completes Step 6.

Figure 8 shows an example of painting the tile pattern of Figure 7.

3 Some Extensions

3.1 Choice of Congenial Tiles

The proposed method can create a Sky and Water pattern for any pair of tiles. However, the smoothness of the transition from the tiles to the background depends heavily on the choice of the shapes of the two tiles, with some transitions being smooth and graceful while others are just mechanical. A smooth transition is more likely to be achieved when we choose the pair in such a way that one tile's shape is very close to the shape of the vacant space surrounded by four copies of the other tile.

As Figure 4 illustrates, our system constructs that vacant space after just one tile is supplied. Once the shape of the vacant space is shown, the user can choose rather easily another tile that is "congenial" with respect to the first one, that is, one which is a good fit to the vacant space.

For example, the tile shown in Figure 9(a) is similar to the shape of the vacant space in Figure 4,

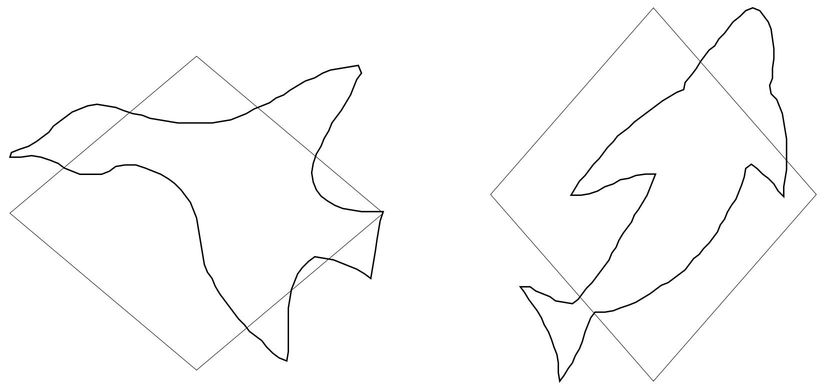

(a) (b)

Figure 9. Congenial and uncongenial tiles with respect to the vacant space in Figure 4.

whereas the tile in Figure 9(b) is not at all close to that shape. Therefore, we can expect the pair of tiles in Figure 3(b) and Figure 9(a) to be congenial, while the pair in Figure 3(b) and Figure 9(b) will not be.

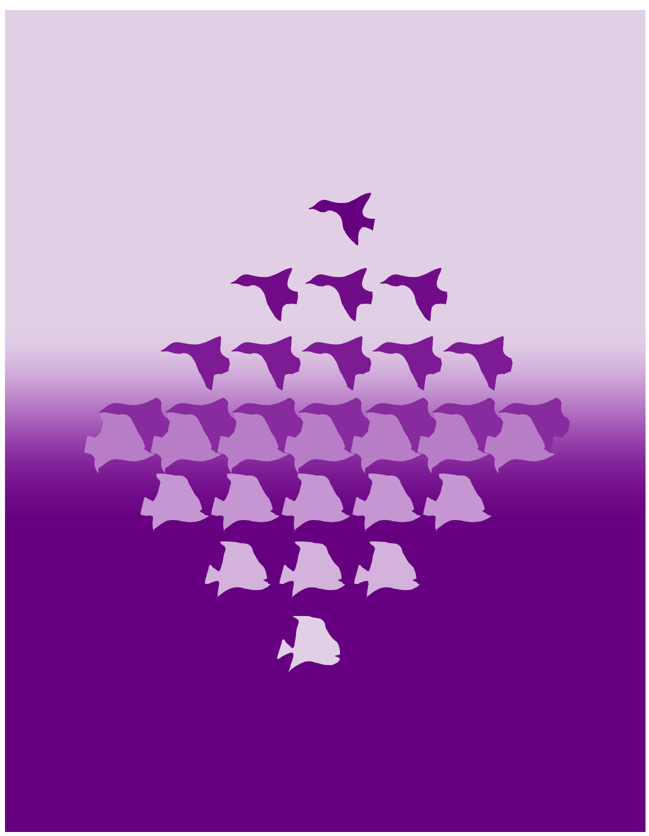

Figure 10. Sky and Water pattern generated by congenial tiles.

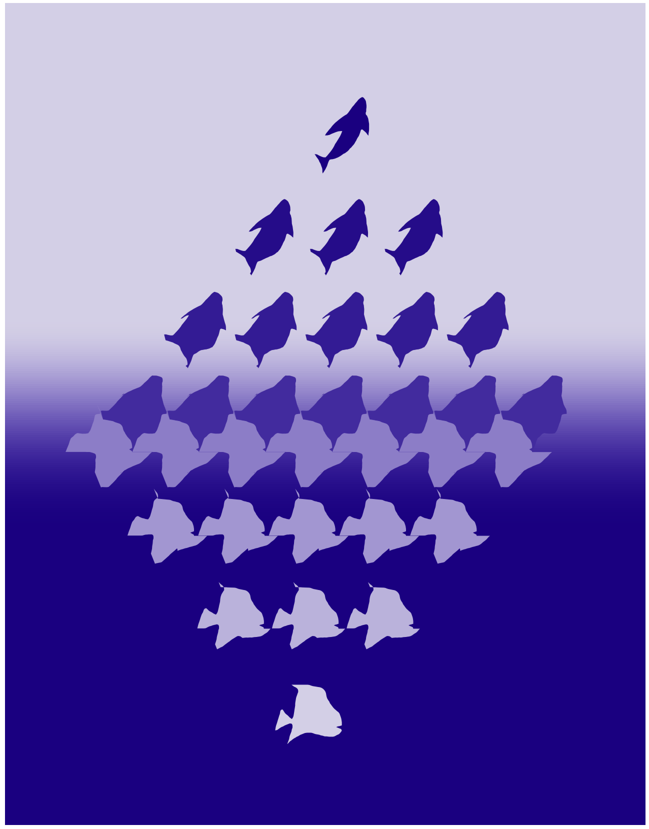

Figure 11. Sky and Water pattern generated by uncongenial tiles.

In fact, the pair in Figure 3(b) and Figure 9(a) produces the Sky and Water pattern shown in Figure 10, and the pair in Figure 3(b) and Figure 9(b) produces the pattern shown in Figure 11. We observe that the transition in Figure 10 is much smoother and more graceful than that in Figure 11, in the sense that the transition from the tiles to the background is more natural.

Therefore, it is important to select the pair of tiles carefully, and the system function that shows the vacant space is useful in enabling users to choose congenial pairs.

3.2 Variations to the Checkerboard Pattern

We used the checkerboard pattern in Figure 2 to deform the tiles vertically from the top downwards. However, we can also use it to deform the tiles horizontally from left to right, as in Escher's print *Day and Night* (1938) [11]. Figure 12 shows an example of this type of pattern, which is generated by our system for a pair of tiles representing a butterfly and a bee.

Other checkerboard patterns can be utilized in a similar manner. Figure 13 shows a vertically deforming tiling pattern based on a parallelogram checkerboard. The composition of the tiling pattern in

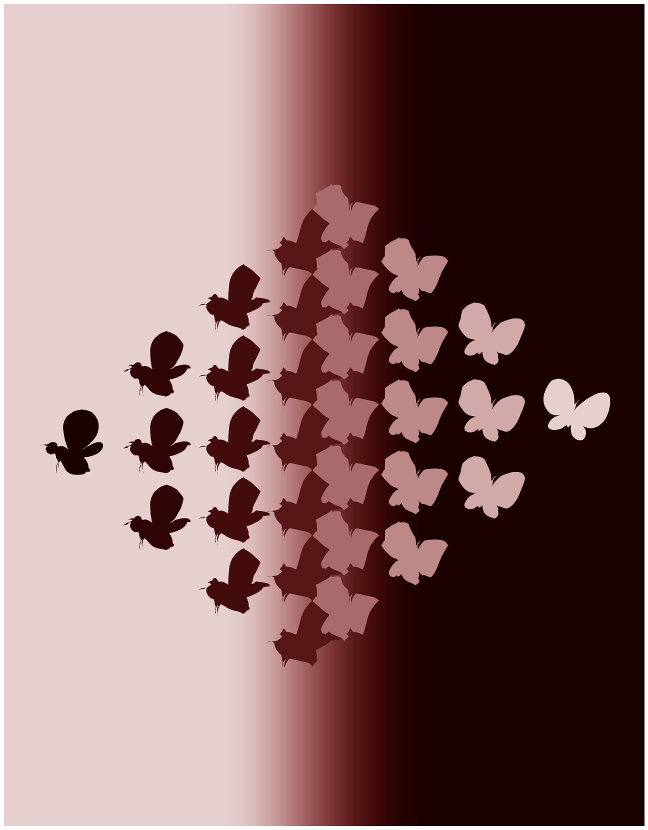

Figure 12. Day and Night pattern generated by a bee and a butterfly.

Figure 13 is somewhat similar to that of Escher's print *Sky and Water II* [11]. In this figure, the steps for generating the tiling patterns are almost the same as those described in Section 2, with the only difference being the shape of the underlying checkerboard grid.

4 Discussion

The algorithm proposed in this paper was inspired by Escher's print *Sky and Water I*, but it is much simpler than Escher's original procedure for creating his print. Therefore, the resulting output of our algorithm is only an approximation of Escher's print, and is not a faithful reproduction of his art, there being many differences in detail. In this section, we compare our algorithm with Escher's work, and discuss the differences.

First, our output pattern, such as that of Figure 8, does not have the same symmetry as Escher's *Sky and Water I* print. In his print, the top bird is in vertical alignment with the bottom fish, whereas, in Figure 8, the bottom fish is one column to the left of a vertical line through the top bird. This is because our underlying checkerboard is not symmetric, with the number of cells in one side differing by one from

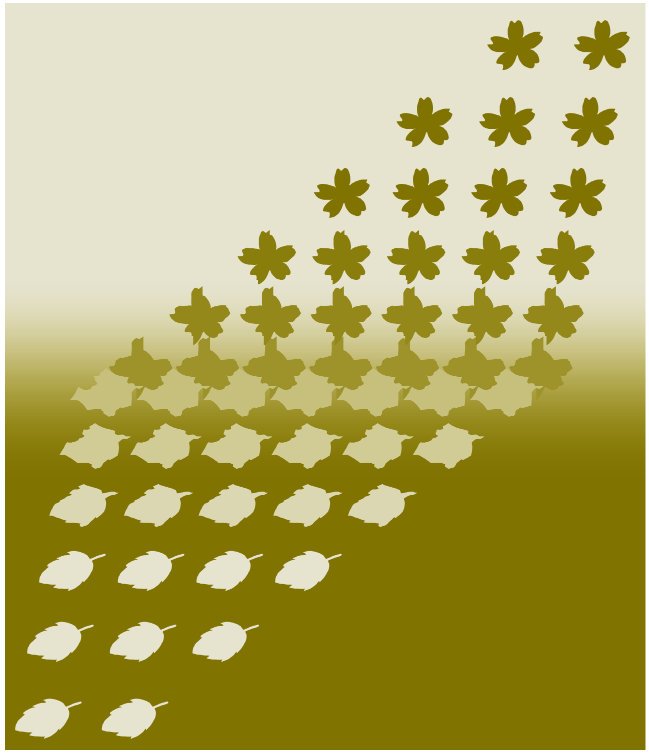

Figure 13. Tiling pattern with a vertical transition, based on a parallelogram checkerboard, and generated by cherry blossom and leaf tiles.

that in the other side.

Escher's more symmetrical effect can be achieved in one of two ways, using our process. First, we could begin with a grid of parallelograms rather than rhombuses, whose n rows and $n+1$ columns outline a rhombus with vertical and horizontal lines of symmetry. Alternatively, we could have followed our method to obtain the tiling pattern in Figure 7 and then applied a horizontal shear to the pattern of tiles, to make the outline of the underlying grid a rhombus with vertical and horizontal lines of symmetry.

In our procedure, we started with an underlying checkerboard of rhomboid cells, but there is some choice in the underlying cell pattern. For example, we might consider using a grid of rectangular cells instead of rhomboid cells, as shown in Figure 14. In this grid, we would also place the rectangular cells in an asymmetric manner, to ensure that the top cell and the bottom cell have different colors. We could achieve Escher's symmetry in a similar way, even starting with this grid pattern. It is not easy to tell which grid is more suitable, Figure 2 or Figure 14.

Another clear difference between our output and Escher's print is that our algorithm generates only silhouettes of the deformed tiles, whereas, in Escher's prints, details within the tiles are also drawn. However, it might not be too difficult to automatically generate these details.

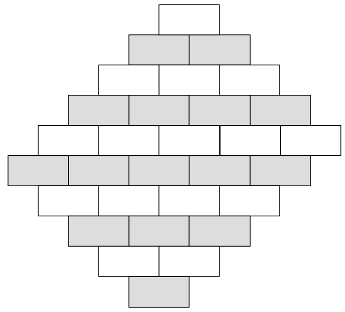

Figure 14. Another possible grid for Sky and Water patterns.

Suppose that the input tiles A and B contain internal details represented by curved lines, in addition to their silhouettes. We can then apply mesh morphing techniques to the tiles. That is, we first approximate the curved lines by polygonal lines, and then generate a triangular mesh inside the tiles in such a way that all the polygonal lines are used as edges of the mesh. Next, we apply mesh morphing, by which the mesh structure is deformed according to the deformation of the boundary (i.e., the tile shape), and collect the deformed edges associated with the details within the tile. In this way, we obtain a deformed version of the details. Finally, we add these deformed details to the corresponding deformed tiles so that the details gradually decrease in contrast and eventually fade out midway through the deformation. In other words, the details within the bird tile are most clear at the top, gradually become less clear downwards, and fade out in the middle row. Similarly, the details within the fish tile are most clear at the bottom, and gradually fade out upwards.

Another difference between our algorithm and Escher's work might be the way the pair of top and bottom tiles are chosen. In our algorithm, an arbitrary pair of tiles can be supplied, and the transition is generated automatically. On the other hand, it seems that Escher aimed for "perfectly congenial" tiles in the middle row. That is, one tile perfectly filled the vacant space formed by the four tiles that surrounded it. He achieved this by beginning with an interlocking periodic tiling of two tiles (a 2-isohedral tiling) in which one tile could serve as the figure while the other tile served as the background [12]. He then used one strip of these interlocking tiles as his starting point, deforming the dark-colored tiles upwards to generate the top tile (tile A in our algorithm), and deforming the light-colored tiles downwards to generate the bottom tile (tile B in our algorithm). Therefore, Escher might have generated the actual top and the bottom tiles at the final stage, whereas they are supplied at the initial stage of our algorithm.

5 Concluding Remarks

We have presented a method for generating Escher-like Sky and Water tiling patterns. In this method, the user supplies a pair of tiles, and the system automatically generates a tiling pattern in which one tile gradually melts away to the background while the other tile gradually appears from the background. This method therefore provides a computer-aided system that enables anyone to create Escher-like Sky and Water tiling patterns easily.

Figure 15. System used in the museum.

A version of this system was placed in the Ehime Prefecture Museum in Matsuyama City, Japan, during the special exhibition of Escher's World held in the summer of 2007. Visitors could use it to create their own Sky and Water patters. Figure 15 shows visitors using the system during the exhibition. We collected comments from users and are using them as feedback to aid revision of the system.

We are considering several directions for further research. One is to extend the method to three or more basic tiles. In his print *Day and Night*, Escher used three basic tiles, a bird flying to the left, a bird flying to the right and a rhombus representing a division of a farmer's field. These tiles deform both horizontally and vertically, thereby generating an interesting tiling pattern. We would like to construct a mathematical method for generating these patterns automatically.

Another direction for extension is altering the checkerboard. In this paper, we used a regular checkerboard with congruent rhombuses as cells. The rhombuses could easily be replaced by congruent parallelograms. However, we could also consider a deformation of the checkerboard itself, such as a checkerboard in which the cell sizes change gradually.

Japanese tessellation artist Makoto Nakamura presents many tiling works in his web page (http://www.k4.dion.ne.jp/˜mnak in which the figure-background reversal is realized in animation. Indeed, deformation of tiles in time is another possibility to realize the figure-background reversal. To construct a computer-aided system for making this kind of animation, particularly deformation of tiles in both space and time, is another interesting direction of future work.

Yet another direction for extension might be the construction of three-dimensional works.

Acknowledgements

The author would like to express his great thanks to Ms. Kyouko Yasuda of Huis ten Bosch and Mr. Koji Endo of the Ehime Prefecture Museum for the opportunity to place the system on public display during the special Escher exhibition, and to the editor of JMA and the anonymous referees for their valuable comments. This work is partly supported by the Grant-in-Aid for Scientific Research (B) No. 20360044 and the Grant-in-Aid for Exploratory Research No. 19650003 of the Japanese Society for Promotion of Science.

References

[1] M. Alexa: Recent advances in mesh morphing. *Computer Graphics Forum*, vol. 21, 2002, pp. 173–197.

[2] L. Cervini, R. Farinato and L. Loreto: The interactive computer graphics (ICG) production of the 17 two-dimensional crystallographic group, and other related topics. In H. S. M. Coxeter et al. (eds.): M. C. Escher—Art and Science, North-Holland, Amsterdam, 1986, pp. 269–284.

[3] H. S. M. Coxeter: Coloured symmetry. In H. S. M. Coxeter et al. (eds.): M. C. Escher—Art and Science, North-Holland, Amsterdam, 1986, pp. 15–33.

[4] M. Emmer: Movies on M. C. Escher and their mathematical appeal. In H. S. M. Coxeter et al. (eds.): M. C. Escher—Art and Science, North-Holland, Amsterdam, 1986, pp. 249–262.

[5] C. Gotsman and V. Surazhsky: Guaranteed intersection-free polygon morphing. *Computer & Graphics*, vol. 25, 2001, pp. 67–75.

[6] B. Grünbaum and G. C. Shephard: *Tilings and Patterns—An Introduction*. W. H. Freeman, New York, 1989.

[7] C. S. Kaplan: Metamorphosis in Escher's art. In *Bridges 2008—Mathematical Connections in Art, Music and Science*, 2008, pp. 39–46.

[8] C. S. Kaplan and D. H. Salesin: Escherization. *Proceedings of SIGGRAPH 2000*, New Orleans, LA, pp. 499–510.

[9] Dihedral Escherization. *Proceedings of Graphics Interface 2004*, May 17–19, London, Ontario, pp. 255–262.

[10] G. E. Martin: *Transformation Geometry—An Introduction to Symmetry.* Springer-Verlag, New York, 1982.

[11] D. Schattschneider: *M. C. Escher—Visions of Symmetry.* New Edition, Abrams, New York, 2004.

[12] D. Schattschneider: Lessons in duality and symmetry from M. C. Escher. In *Bridges 2008—Mathematical Connections in Art, Music and Science*, 2008, pp. 1–8.

[13] G. C. Shephard: What Escher might have done. In H. S. M. Coxeter et al. (eds.): M. C. Escher—Art and Science, North-Holland, Amsterdam, 1986, pp. 111–122.

[14] M. L. Teuber: Perceptual theory and ambiguity in the work of M. C. Escher against the background of 20th Century art. In H. S. M. Coxeter et al. (eds.): M. C. Escher—Art and Science, North-Holland, Amsterdam, 1986, pp. 159–178.